Half plateaus in the linear thermal conductance of quantum point contacts

2004 J. Phys.: Condens. Matter 16 3671

(http://iopscience.iop.org/0953-8984/16/21/015)

INSTITUTE OF PHYSICS PUBLISHING JOURNAL OF PHYSICS: CONDENSED MATTER

J. Phys.: Condens. Matter **16** (2004) 3671–3679 PII: S0953-8984(04)77065-4

Half plateaus in the linear thermal conductance of quantum point contacts

M A Çipiloğlu and S Turgut

Department of Physics, Middle East Technical University, 06531, Ankara, Turkey

Received 26 February 2004
Published 14 May 2004
Online at stacks.iop.org/JPhysCM/16/3671
DOI: 10.1088/0953-8984/16/21/015

Abstract

The linear thermal conductance of a quantum point contact displays a half-plateau structure, almost flat regions appearing close to half-integer multiples of the conductance quantum. This structure is investigated for the saddle-potential model; its behaviour as a function of contact parameters is also investigated. Half plateaus appear when the thermal energy is less than the subband separation and greater than the energy scale over which the transmission probability for a subband changes. The effect arises from the presence of a current node in the energy-resolved heat current, an energy at which the current is zero. When the transmission steps cross the current node as the gate voltage is varied, the heat conductance remains constant, creating the half plateaus, and this happens only for a certain temperature range. It is found that with increasing temperature the half plateaus become wider and flatter, which makes them more pronounced. It is also found that no half plateaus are present at the first step for any parameter values, and this is tied to the effect that the current node is pushed above the first step by the strong Seebeck potential.

1. Introduction

A large number of studies are carried out on the ballistic transport of electrons across quantum point contacts defined by split-gate techniques on (Al, Ga)As heterostructures. An interesting feature of this transport is the quantization of the electrical conductance [1, 2] in multiples of the conductance quantum $2e^2/h$. This phenomenon is usually treated with the Landauer–Büttiker formalism [3, 4], which has a transparent explanation for the quantization. For each transverse mode in the contact, there is in effect a one-dimensional energy subband corresponding to that mode within the contact region. When a subband minimum is sufficiently below the Fermi level, the electrons in that band contribute one quantum $2e^2/h$ to the electrical conductance for adiabatically varying contact potentials, where the factor 2 comes from spin degeneracy. As the voltage on the split gates is varied, the electrical conductance defines smooth plateaus, occasionally changing from one plateau into the other in smooth steps whenever a subband starts to be (un)occupied.

The thermal conductance is also quantized [5–7] in the same way in integer multiples of

$$K_0 = \frac{2\pi^2}{3h} k_B^2 \theta,$$

where θ denotes the temperature. This quantization has exactly the same character as the electrical conductance. The plateaus and steps appear at the same gate voltages. This can simply be understood as a direct result of the Wiedemann–Franz law relating the thermal conductance, K, to the electrical conductance, G, by

$$\frac{K}{\theta G} = \frac{\pi^2 k_B^2}{3e^2},$$

which is seen to remain valid in quantum point contacts although small violations can be observed around steps [5].

A remarkable difference between the curves of the two conductances as a function of gate voltage is the appearance of half plateaus in the thermal conductance, i.e., almost flat regions around half-integral multiples of K_0, which was first noted by van Houten *et al* [6]. To the authors' knowledge, these additional plateaus have not yet been observed experimentally, and there has been no detailed theoretical investigation about them. Similar half-plateau structures have also been observed in the electrical conductance as a result of distinct causes. An applied magnetic field that lifts the spin degeneracy is one possible cause. Also, for finite values of the source–drain voltage (i.e., in the nonlinear regime) a new plateau structure develops at the middle of the steps [8–11]. These plateaus increase in width for increasing source–drain voltage and they eventually obliterate the normal quantization plateaus. However, the half plateaus in the thermal conductance can occur under zero magnetic field and in the linear regime. The purpose of this work is to analyse the half plateaus in the thermal conductance at different temperatures and contact parameters. The theory is summarized in the following section, and after that the conductances are investigated for different parameter values. Finally, a physical explanation for the structure is provided.

2. Theory

If both sides of a quantum point contact have different potentials and temperatures, the charge (I) and the heat ($\dot{Q}$) currents that pass through the contact can be expressed in the linear regime as [12]

$$I = 2\frac{e^2}{h} g_0 V + 2\frac{(-e)k_B}{h} g_1 \Delta\theta, \tag{1}$$

$$\dot{Q} = 2\frac{(-e)k_B\theta}{h} g_1 V + 2\frac{k_B^2\theta}{h} g_2 \Delta\theta, \tag{2}$$

where V is the electric potential difference, $\Delta\theta$ is the temperature difference, and g_p are dimensionless quantities defined as

$$g_p = \int \mathrm{d}x\, x^p (-f'(x)) T(\mu + x k_B \theta), \qquad (p = 0, 1, 2), \tag{3}$$

where μ is the chemical potential, $f(x) = 1/(1+\mathrm{e}^x)$ is the Fermi–Dirac distribution function, and $T(E)$ is the sum of the transmission probabilities at energy E. In other words,

$$T(E) = \sum_n T_n(E),$$

where $T_n(E)$ is the transmission probability of an electron incident in mode n and at the energy E.

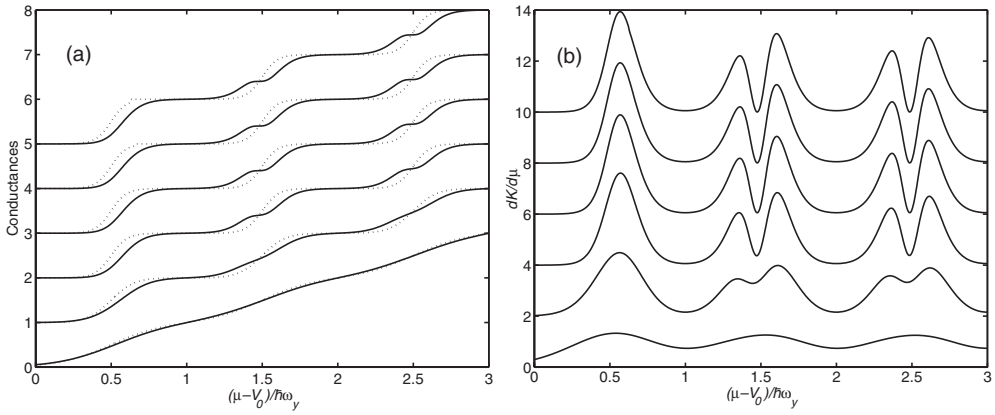

Figure 1. (a) The electrical conductance (dotted) in units of $2e^2/h$ and the thermal conductance (solid) in units of K_0 plotted as a function of the chemical potential. The curves are for (from bottom to top) $\omega_y/\omega_x = 1, 3, 10, 30, 100$ and 300 and $k_B\theta/\hbar\omega_y = 0.05$. The different curves are shifted vertically for the sake of clarity. (b) The derivative of the thermal conductance (in units of $K_0/\hbar\omega_y$) for the same parameter values. The ratio ω_y/ω_x increases from the bottom to the top, and the different curves are shifted vertically by two units.

The electrical conductance, which is measured at isothermal conditions, and the thermal conductance, which is measured at zero electrical current ($I = 0$), are respectively given by

$$G = \frac{2e^2}{h} g_0, \tag{4}$$

$$K = \frac{2k_B^2\theta}{h}\left(g_2 - \frac{g_1^2}{g_0}\right). \tag{5}$$

For calculating the conductances, the saddle potential model [13] is used, where the potential energy around the contact is expressed as

$$V(x, y) = V_0 - \tfrac{1}{2}m\omega_x^2 x^2 + \tfrac{1}{2}m\omega_y^2 y^2, \tag{6}$$

where V_0 refers to the value of the constriction potential at the saddle point, x and y correspond to the longitudinal and transverse directions respectively, and curvatures of the potential are expressed in terms of the frequencies ω_y and ω_x. The transmission probabilities for this potential have been calculated as [14, 15]

$$T_n(E) = \left(1 + \exp\left(-\frac{2\pi}{\hbar\omega_x}(E - E_n)\right)\right)^{-1}$$

for $n = 0, 1, 2, \ldots$, where $E_n = V_0 + \hbar\omega_y(n + 1/2)$. The energy scales for this problem are the subband separation, $E_T = \hbar\omega_y$, and the energy range for a step $E_L \approx \hbar\omega_x$. Physically, a smaller $\hbar\omega_x$ implies that the contact is longer, which results in rapid changes of tunnelling probability with electron energy.

3. Results and discussion

The electrical and thermal conductances are evaluated numerically and plotted in figure 1(a) for different values of the ω_y/ω_x ratio. For large values of ω_x (short contacts) both quantities follow the same curve. But when ω_x becomes smaller (longer contacts), half plateaus in the thermal conductance start appearing, except in the first step. The development of the half

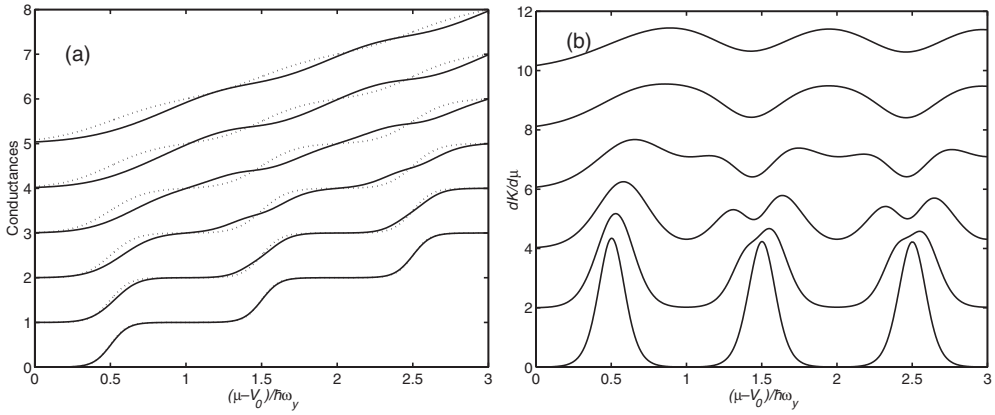

Figure 2. (a) The electrical conductance (dotted) in units of $2e^2/h$ and thermal conductance (solid) in units of K_0 plotted as a function of the chemical potential. The curves are obtained for (from bottom to top) $k_B\theta/\hbar\omega_y = 0.01, 0.03, 0.06, 0.1, 0.15$ and 0.2 and $\omega_y/\omega_x = 3$. The different curves are shifted vertically for the sake of clarity. (b) The derivative of the thermal conductance with respect to chemical potential (in units of $K_0/\hbar\omega_y$) for the same parameter values. The different curves are shifted vertically by two units for clarity, and the temperature increases from the bottom to the top.

plateaus can be seen more clearly in the derivative of the thermal conductance with respect to the chemical potential, which is shown in figure 1(b). For large values of ω_x, the derivative displays only a single peak at each step. When ω_x is decreased, the peaks first split into two, indicating the development of a flatter structure. At smaller values of ω_x, the derivative in between the peaks decreases somewhat, indicating that the structure in the thermal conductance is almost flat. It can be seen from the figures that the widths of these plateaus do not change as ω_x is lowered further.

The appearance of the half-plateau structure can also be seen for increasing temperature, as shown in figure 2. At low temperatures, both conductances follow the same curve as a function of the chemical potential. However, as the temperature is increased, a half-plateau structure becomes apparent for the thermal conductance. When the temperature is increased further, the half plateaus become wider and eventually wipe out the integer plateaus. It can be verified that the width of the secondary plateaus are proportional to the temperature. The obliteration of the integer plateaus becomes inevitable as $k_B\theta$ becomes comparable to $E_T = \hbar\omega_y$. It is interesting to observe that in this parameter range, although the integer plateaus are wiped out, the half-plateau structure is still distinguishable. This can be seen more clearly in the derivative of the thermal conductance in figure 2(b).

The most relevant quantity determining the presence or the absence of the half plateaus appears to be the $k_B\theta/E_L$ ratio. Since, for the saddle-potential model, all steps have the same value for E_L, half plateaus develop concurrently in all steps for a certain range of values of this ratio. There are four different regimes with rough boundaries that can be distinguished in this model. A few representative plots belonging to some of these regimes are shown in figure 3.

(1) In the low temperature regime where $k_B\theta/\hbar\omega_x \lesssim 0.08$, there are no half plateaus. Moreover, the derivative $\partial K/\partial\mu$ has only a single peak at the steps.
(2) In the intermediate temperature regime where $0.08 \lesssim k_B\theta/\hbar\omega_x \lesssim 0.4$, a double-peak structure develops in the derivative $\partial K/\partial\mu$. This is the parameter range where a structure with a smaller slope appears around the middle of the steps in the K versus μ graph. With increasing temperature, that slope goes down, making the graph of K have an almost flat shape at the high end of this regime.

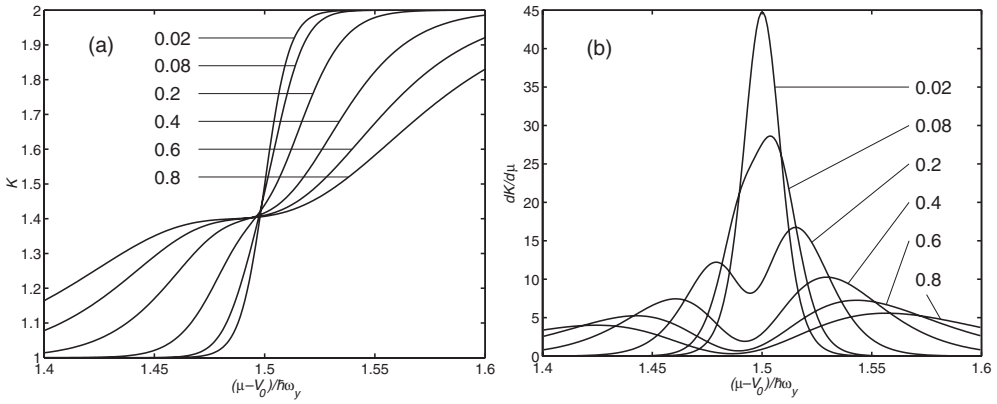

Figure 3. (a) The thermal conductance, K, and (b) its derivative, $\partial K/\partial\mu$, around the second step (the step between $n = 1$ and 2 plateaus) for different values of the $k_B\theta/\hbar\omega_x$ ratio, indicated on the graphs.

(3) In the high temperature regime where $0.4\hbar\omega_x \lesssim k_B\theta \lesssim \hbar\omega_y$, the derivative $\partial K/\partial\mu$ becomes much smaller around the middle of the steps (but does not vanish). As a result, K appears to be almost constant with increasing μ. This is the parameter range where the half plateaus are present. A surprising feature is that the half plateaus become much more pronounced with increasing temperature as a result of the cooperation of two different effects. First, the slope of the plateau region goes further down, and second, the width of that region (i.e., the peak to peak distance in the derivative graph) increases. Since the latter also implies that the widths of the integer plateaus decrease, half plateaus expand at the expense of integer plateaus as the temperature is increased. Towards the high end of this regime, however, neighbouring subbands start contributing to the conduction process, causing the slope of the half plateaus to increase with increasing temperature (not shown).

(4) Finally, at very high temperatures where $k_B\theta \gtrsim \hbar\omega_y$, the contribution of neighbouring subbands is significant, and as a result both integer and half-integer plateaus are wiped out (not shown).

In order to understand the results summarized above, it is necessary to concentrate on the g_2 integral, which is the term in equation (5) that provides the most significant contribution to K. The remaining term, g_1^2/g_0, is essential for including the effect of the Seebeck potential developed across the contact, but its contribution is almost always negligible except around the first step. For this reason, it is appropriate to investigate the derivative of g_2 which can be expressed as

$$\frac{\partial g_2}{\partial\mu} = \int x^2(-f'(x))T'(\mu + xk_B\theta)\,\mathrm{d}x.$$

Here the $x^2(-f'(x))$ factor has a symmetric double-peak shape centred at $x = 0$, with peaks at $x \approx \pm 2.4$ and each peak having a width of order unity. On the other hand, the $T'(\mu + xk_B\theta)$ factor has a single peak at each conductance step with widths of the order $E_L/k_B\theta$. The derivative of g_2 shows the same peak structure as the one of these factors that has the greatest width. Therefore, when $E_L \ll k_B\theta$, $\partial g_2/\partial\mu$ has a double-peak structure at each step, implying the presence of half plateaus, while at the opposite extreme, when $E_L \gg k_B\theta$, it has only a single peak. In the former case, the peak-to-peak distance is around $\Delta\mu = 2 \times 2.4k_B\theta$, which means that the widths of the half plateaus are proportional to the temperature.

The slopes of the half plateaus can also be calculated approximately as follows. To simplify the calculation, consider $\mu = E_n$, which corresponds to the midpoint of the $T = n$ to $n + 1$ transition step. Although the minimum of $\partial K/\partial\mu$ is shifted to lower values of μ as can be seen in figure 3(b), the derivative at the midpoints is sufficient for a rough representative value. Ignoring all other steps for simplicity, which amounts to the approximation $\hbar\omega_y \gg k_B\theta$, one can obtain

$$\frac{\partial g_2}{\partial\mu} = \frac{2\pi}{\hbar\omega_x}\int x^2(-f'(x))(-f'(\lambda x))\,\mathrm{d}x = \frac{2\pi}{\hbar\omega_x}h(\lambda),$$

where $\lambda = 2\pi k_B\theta/\hbar\omega_x$. A limiting value at high temperatures, $k_B\theta \gg \hbar\omega_x$, can be obtained by employing the relation

$$h(\lambda) = \frac{1}{\lambda^3}h\left(\frac{1}{\lambda}\right),$$

as $h(\lambda) \approx h(0)/\lambda^3$, resulting in the following:

$$\frac{\partial g_2}{\partial\mu} \approx \frac{1}{48}\frac{(\hbar\omega_x)^2}{(k_B\theta)^3}.$$

To be complete, the contribution of the terms arising from the Seebeck effect has to be included as well. With a similar analysis it can be found that

$$\frac{1}{K_0}\frac{\partial K}{\partial\mu} \approx \frac{1}{16\pi^2}\frac{(\hbar\omega_x)^2}{(k_B\theta)^3} + \frac{3\ln^2 2}{4\pi^2}\frac{1}{(n+1/2)^2}\frac{1}{k_B\theta}.$$

The restriction $\hbar\omega_y \gg k_B\theta \gg \hbar\omega_x$ and the fact that it gives the slope of only one point on a half plateau makes this expression of limited usefulness for practical cases. The only conclusion that should be drawn from this expression is that in the high-temperature regime where the half plateaus are present, the slope tends to get smaller as the temperature is raised, and it is inversely proportional to the temperature at best. Note that this is very large compared to the slopes of the integer plateaus, which have an exponential dependence on inverse temperature. The main differences between the two types of plateaus comes to light with this result. Half plateaus may not be considered completely flat, but they tend to become flatter as the temperature is raised. In contrast, integer plateaus are considered completely flat when the transmission sum function, $T(E)$, is constant on the plateaus, and this gets better as the temperature is lowered.

Finally, the values of the heat conductance at half plateaus are found not to be exactly equal to the half-integer multiples of the conductance quantum, as can be seen in figure 3(a). Starting from the second step, half plateaus occur at conductance values $K \approx 1.40K_0, 2.44K_0, 3.46K_0$ and so on, approaching half-integer multiples of K_0 as the number of conducting subbands increases. Numerical calculations indicate that these values are independent of all parameters of the problem. For this reason, in order to calculate the values of the conductance, the $\omega_x \to 0$ limit can be considered to simplify the problem. In this limit, $T(E)$ has a step-function dependence on E. When the chemical potential is chosen at the midpoint of $T = n$ to $n + 1$ transition step, the values

$$g_0 = n + \tfrac{1}{2}, \qquad g_1 = \ln 2, \qquad g_2 = \frac{\pi^2}{3}\left(n + \frac{1}{2}\right),$$

can be found, which give the conductance values

$$K = K_0\left(n + \frac{1}{2} - \frac{3\ln^2 2}{\pi^2}\frac{1}{n+\frac{1}{2}}\right) \qquad n = 1, 2, \ldots.$$

Numerically calculated values are consistent with this expression.

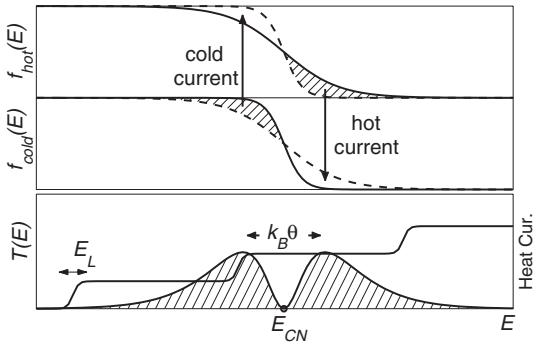

Figure 4. Currents between a hot (top) and a cold conductor (middle). The transmission sum function, $T(E)$, and the energy-resolved heat current (shaded curve) are plotted below. The current node, E_{CN}, the energy at which the current is zero, is present due to the restriction that the total particle current is zero. The relative shift of the Fermi levels due to the Seebeck effect is not shown.

Although the bimodal character of the kernel of the integral for g_2 is responsible for the half plateaus [6], there is a more straightforward explanation that involves uncomplicated physical terms. As illustrated in figure 4, when a hot and a cold conductor are connected so that there is no net electrical current between them, the distribution of electrons has the property that there are more electrons above the Fermi level in the hot conductor compared to the cold one. As a result, at these energies the particle current is from the hot to the cold conductor and they carry more energy than the Fermi energy (hot current). On the other hand, the cold conductor has more electrons with energy less than the Fermi level. For this reason these electrons flow from the cold to the hot conductor and therefore they carry energy smaller than the Fermi energy (cold current). Obviously both currents cause a net heat transfer from the hot to the cold conductor. The important point is that in between them there is some energy where there is no particle current. Note that there should inevitably be such a current node if the zero net electric current condition is satisfied, which is always the case for heat conductance measurements. Finally, when the gate voltage on the contact is changed, the transmission probabilities and the currents are altered. The two relevant energy scales are E_{L}, the energy range where the transmission probability is modified for small changes in the gate voltage, and $k_{\mathrm{B}}\theta$, the distance between the hot and cold current energies. In the case $E_{\mathrm{L}} \ll k_{\mathrm{B}}\theta$, when the modification region crosses through the current node, the thermal current remains constant, creating the half-plateau structure of the thermal conductance. It also follows from this argument that the width of the plateaus is proportional to the temperature. In the opposite case, $E_{\mathrm{L}} \gtrsim k_{\mathrm{B}}\theta$, the current node cannot be resolved from the current peaks, and no half plateaus appear.

In the argument above, the relative shift of the Fermi levels due to the Seebeck effect has to be taken into the account, as it will move the current node away from the Fermi level. However, as long as the node does not deviate too much, the crossing of the node with steps is inevitable. This appears to be the case for the second and higher steps, but not for the first one. In the case of the first step, only a negligible amount of current flows at electron energies E with $T(E) \approx 0$. The significant part of the current should flow at higher energies on the $T(E) \approx 1$ side of the step. The current node is necessarily pushed above the first step, and for this reason crossing does not occur, which explains why there are no half plateaus at the first step. In order to quantify this idea, the current node energy is calculated. Starting from the current expression between energies E and $E + \mathrm{d}E$ in the linear regime,

$$(f_{\mathrm{hot}}(E) - f_{\mathrm{cold}}(E))T(E)\,\mathrm{d}E = \left(\frac{\partial f(E)}{\partial \mu}(-e)V + \frac{\partial f(E)}{\partial \theta}\Delta\theta\right)\mathrm{d}E,$$

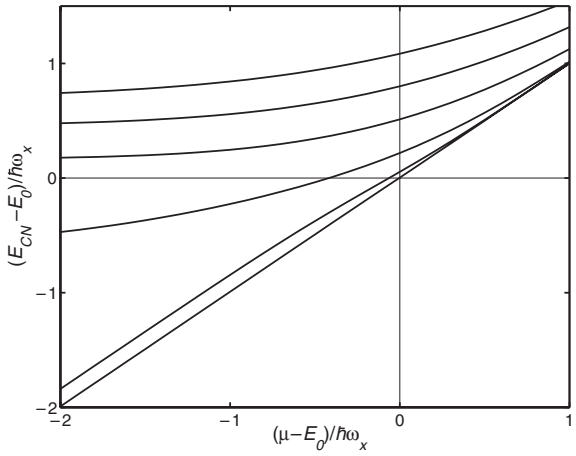

Figure 5. The energy of the current node as a function of the chemical potential for the first step. The effects of the other steps are ignored (i.e., $\omega_y \gg \omega_x$). The curves are obtained for (from bottom to top) $k_B\theta/\hbar\omega_x = 0.02, 0.08, 0.2, 0.4, 0.6$ and 0.8. For the lowest curve, E_{CN} is roughly equal to μ.

and using the Seebeck coefficient, $V/\Delta\theta = k_B g_1/e g_0$, one can obtain the energy of the current node as

$$E_{CN} = \mu + k_B\theta\frac{g_1}{g_0}.$$

Half plateaus occur when this energy and the subband minima cross, i.e., when $E_{CN} \sim E_n$. As can be seen, the current node deviates from the Fermi level only by an amount proportional to the Seebeck coefficient. It is well known that the Seebeck coefficient displays peaks at the steps and minima at the plateaus; however, it is large and non-zero at and below the first step [6]. For this reason, the deviation of the current node becomes very important in this last case, which can be seen in figure 5, where E_{CN} is plotted around the first step ($n = 0$). Although for low temperatures ($k_B\theta/\hbar\omega_x = 0.02$, 0.8 and 0.2) the current node does not deviate much from the Fermi level and it indeed crosses the step (E_{CN} becomes smaller than E_0), these cases belong to the low and intermediate temperature regimes where the half plateaus are not observed. For high temperatures where there should have been half plateaus, however ($k_B\theta/\hbar\omega_x = 0.4$, 0.6 and 0.8), the Seebeck effect pushes E_{CN} significantly above the Fermi level, with the result that E_{CN} also lies above the subband minimum, E_0. Therefore, no crossing occurs at energies around the step, and for this reason there is no half plateau. Although it is found that E_{CN} gets smaller with decreasing μ and it eventually crosses E_0, this happens for much lower values of μ, so that practically there is no current flowing. In summary, for all parameter ranges there cannot be any half plateau on the first step either because the temperature is too small so that the current node is not resolved, or because the current node cannot cross the step. Indeed, no unusual structure has been observed at this step either in K or in $\partial K/\partial\mu$ for all parameters that are investigated in this numerical study.

4. Conclusions

The formation and evolution of half-plateau structures in the thermal conductance are described. They are the most significant aspect of the violation of the Wiedemann–Franz law. The thermal distribution of energies of electrons contributing to a conduction process has a single-peak shape for electrical conductance measurements. In contrast, for thermal

conductance measurements, it has a double-peak shape. If the transmission probability of a quantum point contact changes rapidly with electron energy, the conductances become sensitive to the details of that distribution. The appearance of half plateaus in the thermal conductance is the most important result of that sensitivity.

The half plateaus appear in the temperature range $E_{\mathrm{L}} \lesssim k_{\mathrm{B}}\theta \lesssim E_{\mathrm{T}}$. For this reason, a long contact with a smaller value of E_{L} increases the chances of experimental observation. Interestingly, half plateaus become more pronounced as the temperature is raised, as they get wider and less steep at the low end of the temperature range above. Around $k_{\mathrm{B}}\theta \sim E_{\mathrm{T}}$, they start disappearing together with the integer plateaus, but due to their widths they are a little bit more distinguishable. The values of the conductance at the half plateaus are also evaluated and it is observed that these values are fixed, independent of the parameters of the contact. Although they are smaller than the exact half-integer multiples of the conductance quantum, they tend to approach these values as the subband index increases. Finally, due to the strong effect of the Seebeck potential developed across the contact, no half plateaus appear at the first step for any parameter values.

References

[1] van Wees B J, van Houten H, Beenakker C W J, Williamson J G, Kouwenhoven L P, van der Marel D and Foxon C T 1988 *Phys. Rev. Lett.* **60** 848

[2] Wharam D A, Thornton T J, Newbury R, Pepper M, Ahmed H, Frost J E F, Hasko D G, Peacock D C, Ritchie D A and Jones G A C 1988 *J. Phys. C: Solid State Phys.* **21** L209

[3] Landauer R 1970 *Phil. Mag.* **21** 863

[4] Büttiker M, Imry Y, Landauer R and Pinhas S 1985 *Phys. Rev.* B **31** 6207

[5] Preotto C R 1991 *Solid State Commun.* **80** 909

[6] van Houten H, Molenkamp L W, Beenakker C W J and Foxon C T 1992 *Semicond. Sci. Technol.* **7** B215

[7] Molenkamp L W, Gravier Th, van Houten H, Buijk O J A, Mabesoone M A A and Foxon C T 1992 *Phys. Rev. Lett.* **68** 3765

[8] Glazman L I and Khaetskii A V 1989 *Europhys. Lett.* **9** 263

[9] Xu H 1993 *Phys. Rev.* B **47** 15630

[10] Patel N K, Nicholls J T, MartínMoreno L, Pepper M, Frost J E F, Ritchie D A and Jones G A C 1991 *Phys. Rev.* B **44** 13549

[11] Frost J E F, Berggren K F, Pepper M, Grimshaw M, Ritchie D A, Churchill A C and Jones G A C 1994 *Phys. Rev.* B **49** 11500

[12] Sivan U and Imry Y 1986 *Phys. Rev.* B **33** 551

[13] Büttiker M 1989 *Phys. Rev.* B **41** 7906

[14] Connor J N L 1968 *Mol. Phys.* **15** 37

[15] Fertig H A and Halperin B I 1987 *Phys. Rev.* B **36** 7969